JOURNAL OF OPTOELECTRONICS AND ADVANCED MATERIALS Vol. 9, No. 8, August 2007, p. 2308 - 2311

Research of superlensing in a honeycomb lattice photonic crystal

DAN LUO*, JIPING NING, QUN HAN, ZHIQIANG CHEN, LIANJU SHANG, GUOFANG FAN
Photoelectronic Information Science & Technology Laboratory, MOE, College of Precision Instruments & Optoelectronics Engineering, Tianjin University, Tianjin 300072, China

The problem of imaging in a honeycomb lattice photonic crystal (PhC) slab is studied theoretically. Also, the superlens imaging of two sources separated by a distance less than a wavelength is shown. The finite-difference time-domain (FDTD) method is employed to investigate the unique feature of imaging of such PhC slab. Specially, it is shown that the surface termination is important for obtaining good imaging quality in honeycomb PhC slab.

(Received February 9, 2007; accepted June 27, 2007)

Keywords: Superlens, Photonic crystal slab, Surface termination, FDTD

1. Introduction

Negative refraction of electromagnetic waves by a left-handed material (LHM) which is characterized by simultaneous negative permittivity and permeability was predicted by Veselago [1] in 1968 to occur in a homogenous medium. The recent discovery of left-handed metamaterials[2,3] has attracted a great deal of interest in this area. Based on the idea of Veselago, Pendry predicted that a lossless LHM slab can amplify evanescent waves, which are responsible for the subwavelength details of source geometry, and thus act as a perfect lens [4]. This LHM slab possesses some advantages over conventional lenses. For example, it can overcome the traditional limitation on lens performance and focus light onto an area smaller than a square wavelength to achieve subwavelength imaging. Since such materials do not exist naturally, proposals have been put forth in recent years to artificially synthesize them [3,5-7]. an effective medium made of metallic rods, and the so-called split-ring resonators, has been shown to act as such a metamedium in the microwave frequency range.

Recently it has been shown that a two-dimensional photonic crystal (2D-PhC) can act as a metamedium [8-10]. Notomi [8] studied light propagation in strongly modulated 2D-PhC, and a negative n_{eff} for a frequency range was found. Further, Luo et al. [11] have shown that the propagation of light in a square 2D-PC in the first photonic band leads to an all angle negative refraction (AANR), which leads to superlensing. Other explorations [12,13] indicated that the surface termination of the photonic crystal slab is important for obtaining a good quality imaging, but the investigations were just developed in square and triangular 2D photonic crystals. In addition, R. Gajić et al [14] studied the all-angle negative refraction in 2D honeycomb lattices made of dielectric rods in air. It was shown that the honeycomb lattice has circle-like equifrequency contours and the effective indices are close to -1 for a wide range of incident angles and frequencies, and the AANR is present for low normalized frequencies which eliminates undesired diffraction. So, it is a good choice to use a honeycomb lattice photonic crystal slab to make a superlensing.

In this paper, we investigate the superlens imaging in a honeycomb lattice photonic crystal slab. The influence of the air-PhC interface on the image quality is also studied. A finite-difference time-domain (FDTD) method[15] with perfectly matched layer boundary conditions [18] is used to obtain the maps of propagating waves through the honeycomb lattice PhC slab.

2. Numerical method

For a linear isotropic material in a source-free region, the time-dependent Maxwell's equations can be written in the form:

$$\frac{\partial \vec{H}}{\partial t} = -\frac{1}{\mu}\nabla \times \vec{E} \tag{1}$$

$$\frac{\partial \vec{E}}{\partial t} = \frac{1}{\varepsilon(\vec{r})}\nabla \times \vec{H} - \frac{\sigma(\vec{r})}{\varepsilon(\vec{r})}\vec{E} \tag{2}$$

where $\varepsilon(\vec{r})$, $\mu(\vec{r})$ and $\sigma(\vec{r})$ are the position dependent permittivity, permeability and conductivity of the material, respectively.

The FDTD method discretizes space and time by replacing the partial derivatives in Maxwell's equations with the centred finite differences using a so-called Yee-cell technique [15,16]. In a two-dimensional photonic crystal (in the x-y plane), electromagnetic fields can be decoupled into the transverse electric (TE) mode and the transverse magnetic (TM) mode [17]. In this paper, only the case of TM mode is studied, so H_z E_x and E_y components are zero, the Maxwell's equations can be described in the following form:

$$\frac{\partial H_x}{\partial t} = -\frac{1}{\mu(\vec{r})}\frac{\partial E_z}{\partial y} \quad (3)$$

$$\frac{\partial H_y}{\partial t} = \frac{1}{\mu(\vec{r})}\frac{\partial E_z}{\partial x} \quad (4)$$

$$\frac{\partial E_z}{\partial t} = \frac{1}{\varepsilon(\vec{r})}[\frac{\partial H_y}{\partial x} - \frac{\partial H_x}{\partial y} - \sigma(\vec{r})E_z] \quad (5)$$

Each unit cell contains 3600 (60 × 60) grid points, which makes sure good result. The time step is chosen to be $\Delta t = 0.95 / c(\Delta x^{-2} + \Delta y^{-2})^{1/2}$, where c is the speed of light, Δx and Δy is space intervals in x and y directions, respectively. In our numerical simulations, the finite-difference time-domain (FDTD) method with perfectly matched layer boundary conditions is used.

3. Results and discussion

A two-dimensional (2D) honeycomb lattice photonic crystal consisting of an array of parallel dielectric cylinders placed in air is considered. The corresponding superlensing system with coordinates is shown in Fig.1, where the δx is the surface termination of the photonic crystal slab on each interface. We choose parameters of Ref.14, i.e., the lattice constant and the radius are, respectively, a and $r = 0.24a$, and the dielectric constant of the cylinders is $\varepsilon = 12.96$ (GaAs). The normalized frequency $f = a/\lambda = 0.22$ within the AANR, which occurs in the TM2 band, is used in this paper. Only the transverse magnetic modes (TM) are considered here. Since the effective refractive index of the honeycomb lattice photonic crystal equal -1, the refraction of light follows simple rules of geometric optics with the Snell's law refraction at each interface, therefore the superlensing is unrestricted [19], which means the position of the image changes for various positions of the point source when keeping a constant thickness of the slab. Fig. 2 shows the propagation maps for this case. We can see that when the distance between the left interface of the slab and the source changes, the distance between the right interface of the slab and the image correspondingly changes.

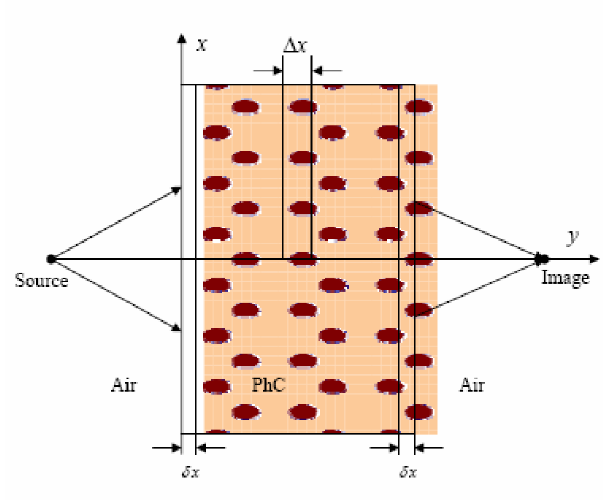

Fig. 1. Schematic diagram of the imaging system formed by a honeycomb lattice photonic crystal slab. The surface termination of the slab is denoted by δx .

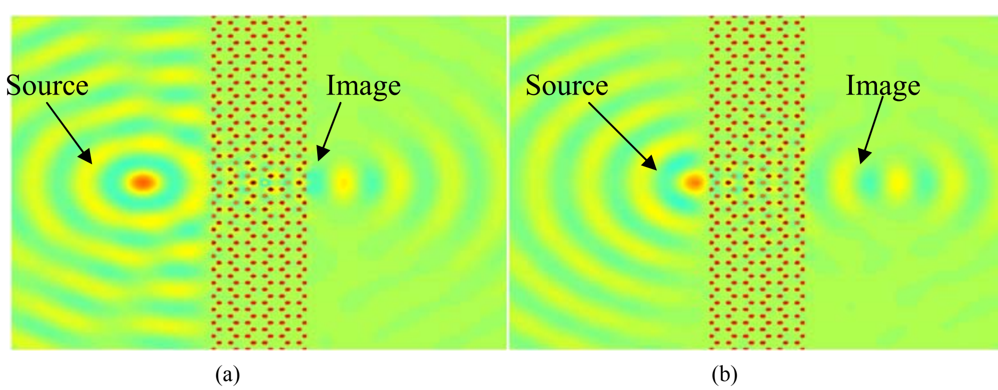

Fig. 2. The propagation map (electric field distribution across space) of the 2D honeycomb lattice photonic crystal slab, for different source position. The frequency is $f = a/\lambda = 0.22$ within the AANR. Positions of the image follow the geometric optics analysis, and Snell's law refraction occurs at each interface.

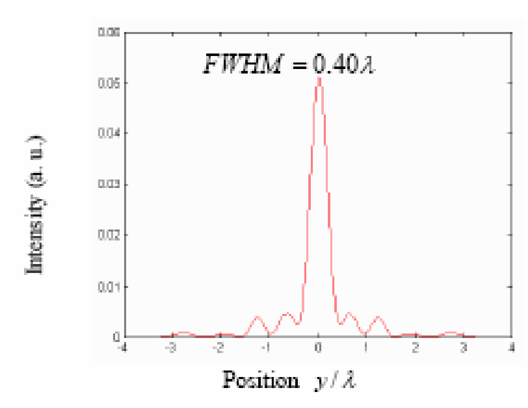

Fig. 3. Light intensity across the image plane of a point source.

In order to demonstrate the superlens imaging, firstly we calculated the $FWHM$ of the image plane of a point source, here $\delta x = 0.71a$ is chosen for achieving good quality of the image, and the effect of surface termination of the PhC slab will be discussed later. Fig. 3 shows the light intensity across the image plane of a point source where $FWHM = 0.40\lambda$, and we find that the subwavelength focusing is observed here. Then, we show the wave propagation map for a two-point source which has the same time dependence in Fig. 4. From this figure it is noted that the image peaks reproduce the source peaks well, which reflects a good resolution of the PhC slab. Here, the two sources are separated by $\Delta y = 0.9\lambda$ and $\delta x = 0.71a$ is chosen. By reducing the between the two point sources well below the wavelength, we can test the possibility of the subwavelength resolution. The map of electric field intensity across the image plane of two point sources with different distance between the sources is shown in Fig. 5.

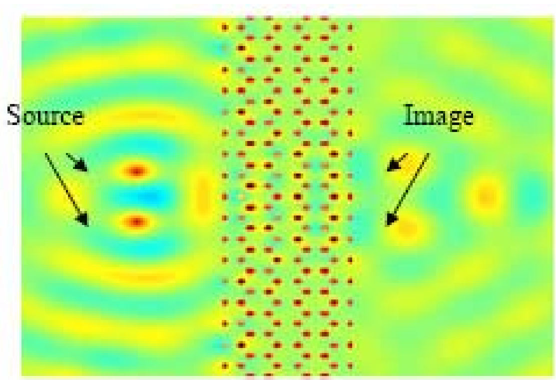

Fig. 4. The propagation map (electric field distribution across space) of a two-point source and its image formed by a honeycomb lattice photonic crystal slab with the distance between the sources $\Delta y = 0.9\lambda$.

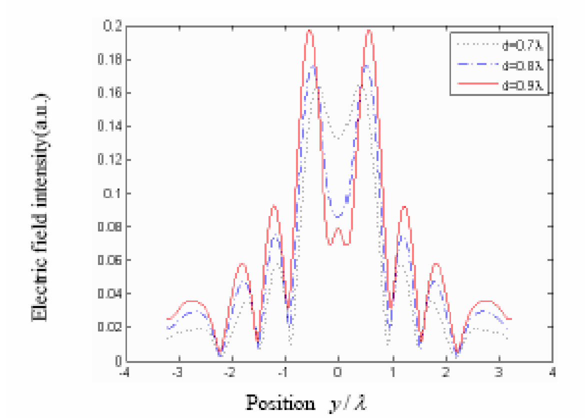

Fig. 5. Electric field intensity across the image plane for three different distances between sources.

It should be noted that the optical properly of a photonic crystal with $n_{eff} = -1$ is different from that of a negative index material with refractive index $n = -1$. For a negative index material (NIM) with $n = -1$, light can go through an air-NIM interface without reflection [4].One can find a different behavior at the interface between air and a PhC slab with $n_{eff} = -1$. In this case, the surface termination of the PhC slab becomes an important parameter, which influences the image quality. Fig. 6 gives the image's electric field intensity as a function of the surface termination δx where a point source of continuous wave is placed at the left side of the photonic crystal slab. It is clearly noted that the electric field intensity of the image is strongly dependant on the surface termination δx . The electric field intensity of the image reaches its maximum values when $\delta x = 0.15a$ and $\delta x = 0.71a$. However, it decreases as δx moves away from these two values. These results are different from previous simulations obtained from triangular and square lattice 2D photonic crystal slabs, where the good image quality occurs when $\delta x = 0.5r$ [12,20]. However, in our simulation of the honeycomb lattice photonic crystal slab, the good image quality appears at $\delta x = 0.15a$ and $\delta x = 0.71a$ (the distance between the centers of the two nearest arrays dielectric materials along the x direction is $\Delta x = 0.5a$ shown in Fig. 1, the length of removed dielectric material here can be treated to be $\delta x' = 0.21a$), respectively, the length of removed dielectric materials at the x direction is more than $0.5r = 0.12a$. It means that the honeycomb lattice photonic crystal slab has special property which is different to the square and triangular lattice photonic crystal slabs. These differences may arise from different structures of photonic crystals. Fig. 7a and Fig. 7b show the snap shots of the electric field for $\delta x = 0$ and $\delta x = 0.15a$, respectively. Fig. 7c and Fig. 7d show the snap shots of the electric field for $\delta x = 0.5a$ and $\delta x = 0.71a$, respectively. However, in

Fig. 7a and Fig. 7c, the images are relatively blurred which indicates that the reflectivity at the air-PhC interface is relatively high. It can be noted that better images are achieved in Fig. 7b ($\delta x = 0.15a$) and Fig. 7d ($\delta x = 0.71a$) comparing to the cases of Fig. 7a ($\delta x = 0$) and Fig. 7c ($\delta x = 0.5a$). The position of the surface termination greatly influences the reflection at the interface between the air and the PhC slab. We also calculate the electric field intensity distribution on the image plane for different slab lengths and find that the influence of the slab length is not as obvious as reported in the case of square lattice PhC slab [18]. It means that the slab length is not an important parameter for the subwavelength resolution in the honeycomb lattice photonic crystal superlens.

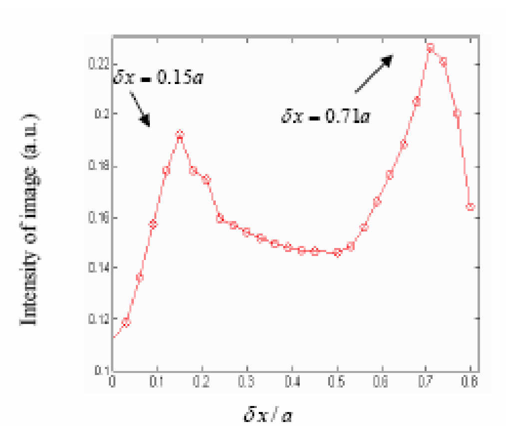

Fig. 6. The electric field intensity of image as function of the surface termination.

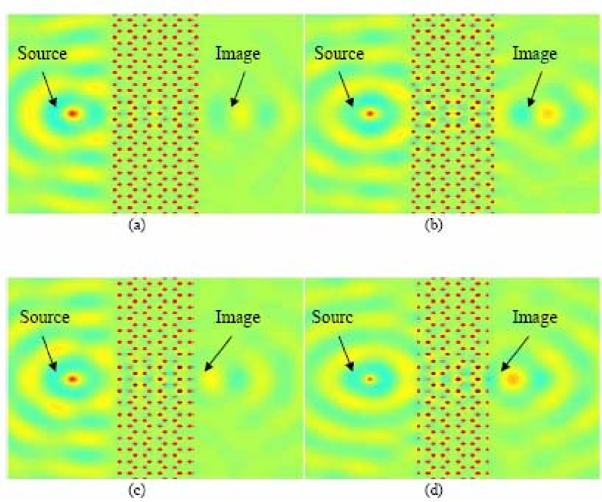

Fig. 7. The propagation map of the electric field of a point source and its image formed by a honeycomb photonic crystal slab with surface of (a) $\delta x = 0$; (b) $\delta x = 0.15a$; (c) $\delta x = 0.5a$; (d) $\delta x = 0.71a$.

4. Conclusion

The finite-difference time-domain method has been employed to investigate the image properties of a 2D-PhC slab. The subwavelength imaging of two-point source with distances between the sources below the wavelength is also shown, which confirm that the honeycomb lattice photonic crystal slab with $n_{eff} = -1$ can act as a superlens. The surface termination of the photonic crystal slab is shown to be an important parameter for obtaining a good quality image, and the honeycomb PhC slab show properties which are different from the square and triangular lattice photonic crystals.

References

[1] V. G. Veselago, Soviet Phys. USPEKHI **10**, 509-514 (1968).

[2] D. R. Smith, W. J. Padilla, D. C. Vier, S. C. Nemat-Nasser, S. Schultz, Phys. Rev. Lett **84**, 4184-4187 (2000).

[3] R. A. Shelby, D. R. Smith, S. Schultz, Science **292**, 77-79 (2001).

[4] J. B. Pendry, Phys. Rev. Lett **85**, 3966-3969 (2000).

[5] J. B. Pendry, A. J. Holden, D. J. Robbins, W. J. Stewart, IEEE Trans. Microwave Theory Tech **47**, 2075-2084 (1999).

[6] J. B. Pendry, A. J. Holden, W. J. Stewart, I. Youngs, Phys. Rev. Lett **76**, 4773-4776 (1996).

[7] D. R. Smith, W. J. Padilla, D. C. Vier, S. C. Nemat-Nasser, S. Schultz, Phys. Rev. Lett **84**, 4184-4187 (2000).

[8] M. Notomi, Phys. Rev. B **62**, 10696-10705 (2000).

[9] S. Foteinopoulou, E. N. Economou, C. M. Soukoulis, Phys. Rev. Lett **90**, 107402 (2003).

[10] S. Foteinopoulou, C. M. Soukoulis, Phys. Rev. B **67**, 235107 (2003).

[11] C. Luo, S. G. Johnson, J. D. Joannopoulos, J. B. Pendry, Phys. Rev. B **65**, 201104 (2002).

[12] S. S. Xiao, M. Qiu, Z. C. Ruan, S. L. He, Appl. Phys. Lett **85**, 4269-4271 (2004).

[13] X. D. Zhang, Phys. Rev. B **71**, 165116 (2005).

[14] R. Gaji, R. Meisels, F. Kuchar, K. Hingerl, Phys. Rev. B **73**, 165310 (2006).

[15] K. S. Yee, IEEE Trans. Antennas Propag **14**, 302-307 (1966).

[16] A. Taflove, Computational Electrodynamics: The Finite-Difference Time-Domain Method.-2nd ed, Artech House, Norwood, 2000.

[17] J. D. Joannopoulos, R. D. Meade, J. N. Winn, Photonic Crystal, Princeton University, Princeton, NJ, 1995.

[18] J. Berenger, J. Comput. Phys **114**, 185-200 (1994).

[19] X. Wang, Z. F. Ren, K. Kempa, Opt. Express **12**, 2919-2924 (2004).

[20] F. AbdelMalek, W. Belhadj, H. Bouchriha, Photon. Nano. Fund. Appl 3, 19-24 (2005).

*Corresponding author: luodan1229@yahoo.com.cn